Dalton Transactions

PAPER

View Article Online
View Journal | View Issue

Cite this: *Dalton Trans.*, 2017, **46**, 16089

Characterization of ammonia binding to the second coordination shell of the oxygen-evolving complex of photosystem II†

Manoj Mandal,[a] Mikhail Askerka,[b] Gourab Banerjee,[b] Muhammed Amin,[c] Gary W. Brudvig,[b] Victor S. Batista[b] and M. R. Gunner*[a]

Received 16th October 2017,
Accepted 3rd November 2017

DOI: 10.1039/c7dt03901h

rsc.li/dalton

The second-shell ammonia binding sites near the OEC (oxygen-evolving complex) of PSII are characterized by combined Continuum Electrostatic/Monte Carlo (MCCE), QM/MM and DFT calculations and compared with new and earlier experimental measurements. MCCE shows ammonia has significant affinity at 6 positions but only two significantly influence the OEC. Although the pK_a of ammonium ion is 9.25, it is calculated to only bind as NH_3, in agreement with its low affinity at low pH. The calculations also help explain the experimentally observed competitive binding of ammonia with chloride. Ammonia and Cl^- compete for one site. Electrostatic interactions cause Cl^- to effect ammonia at two other sites. Cl^- stabilizes the multiline g = 2.0 form of the S_2 state (OEC Mn oxidation state 3444) while ammonia only binds in the g = 4.1 form of the S_2 state (oxidation state 4443) due to the movement of the positive charge between Mn1 and Mn4. One ammonia binds near Mn4 and shares a proton with D2-K317, making the ion pair NH_4^+K317^{0}D61$^-$, making ammonia binding sensitive to the K317A mutation. The affinity of ammonia is also dependent on the protonation state of water 2, a primary ligand to Mn4.

Introduction

Photosynthesis is the process by which green plants, algae and cyanobacteria use the energy of light to produce glucose and oxygen from carbon dioxide and water. There are two light activated protein complexes, Photosystem I (PSI) and Photosystem II (PSII). Virtually all atmospheric molecular oxygen on Earth has been produced by PSII. The difficult redox chemistry of oxidizing water to oxygen is carried out by the Oxygen-Evolving Complex (OEC) a Mn_4O_5Ca cluster.[1] Absorption of photons leads to oxidation of P_{680} in PSII. Electrons are withdrawn from the OEC to reduce P_{680}^+. Four excitations of PSII build up four holes in the OEC, with each of the 4 Mn in the OEC sequentially oxidized from +3 to +4.[2] Proton loss is generally coupled to the OEC oxidation to ensure that the net positive charge does not substantially increase. S_0 is the most reduced and S_3 the most oxidized state. Following formation of S_3 four electrons are removed from two waters in the transient S_4 state, reducing the OEC back to S_0 and O_2 is released. In the course of the S-state cycle, four protons are released to the lumen, adding to the transmembrane electrochemical gradient.

The OEC oxidizes water with earth abundant metals at physiological pH. The study of this process continues to provide insight into how to harness solar energy.[3–5] However, the detailed mechanism for forming oxygen by the OEC remains elusive.[6–10] The identity of the substrate water molecules that form O_2 has yet to be established. It has been proposed that either the terminal waters (W2 on Mn4 and W3 on Ca^{2+}) form O_2,[11,12] or an additional water bound to Mn1 in the S_2 to S_3 state transition reacts with an oxide (O5) bridging two Mn centers to make the O–O bond.[6] The interaction of ammonia, an electronic and structural analogue of water, with the OEC,[13] provides insights into possible mechanisms for substrate water binding.[14–17] Ammonia has two binding sites. In its secondary binding site near the OEC, it inhibits the $S_2 \rightarrow S_3$ transition.[14,18] Recent EPR and QM/MM studies suggested that the secondary ammonia binds near D61 and the nearby Mn4 W1 ligand.[19] It has been proposed that ammonia moves into the primary site in the S_2 state, binding as an additional ligand to the oxidized Mn4, which may be analogous to substrate water binding.[7,20]

The binding site of the secondary ammonia and the mechanism by which it affects the OEC behavior have been the

[a]*Department of Physics, City College of New York, C.U.N.Y. New York 10031, USA. E-mail: marilyn.gunner@gmail.com, mgunner@ccny.cuny.edu*
[b]*Department of Chemistry, Yale University, New Haven, Connecticut 06520, USA*
[c]*Center for Free-Electron Laser Science (CFEL), Deutsches Elektronen-Synchrotron DESY, 22607 Hamburg, Germany*

†Electronic supplementary information (ESI) available. See DOI: 10.1039/c7dt03901h

subject of earlier studies[14,18] but significant issues remain unresolved. With a pK_a of 9.25, ammonia is predominantly NH_4^+ at the pH of 6.0–7.5 at which most experiments are carried out. One surprising experimental finding is that the anionic Cl^- competes with ammonia. Chloride is an essential cofactor, required for progression to the S_3 state.[1,21–24] There are two chlorides near the OEC in X-ray crystal structures: one near K317 and the other near N338 and F339.[1] Cl^- has been proposed to play several roles, including regulating the redox properties of the Mn cluster[25] and blocking formation of a salt bridge between D61 and D2-K317 that can close the proton exit channel.[24,26,27] The D2-K317A mutant was shown to lose sensitivity to either ammonia addition or to Cl^- depletion, suggesting both chloride and ammonia may bind near this Lys.[19,28]

Ammonia and chloride have opposing effects on the OEC S_2 state. For example, there are two spin isomers of the S_2 state with different redox states of the Mn ions in the Mn_4O_5Ca cluster.[29] A multiline EPR signal at $g = 2$ with spin $\frac{1}{2}$ has Mn4, closest to the Cl^-, oxidized (redox state 3444 indicates $Mn1^{3+}Mn2^{4+}Mn3^{4+}Mn4^{4+}$). The other has an overall spin of 5/2 and an EPR signal at $g = 4.1$ that is associated with oxidation of Mn1, which is farthest from the Cl^- (redox state 4443). Cl^- stabilizes the S_2 $g = 2.0$ state, while the secondary ammonia binding stabilizes the high spin S_2 $g = 4.1$ state.[14,18,19,30,31]

Here, we combine Monte Carlo sampling with continuum electrostatics and molecular mechanics energies (MCCE[32]) with DFT and QM/MM analysis to explore the behavior of the secondary ammonia. New experimental results characterize the pH dependence of binding. Calculations assess multiple potential sites for ammonia binding to determine why the ammonia affinity depends on the Cl^- concentration, pH, the S_2-spin isomer and the presence of the wild-type Lys or mutated Ala at position D2-K317. The position and protonation state of ammonia are allowed to remain in equilibrium with the protein protonation state, Cl^- occupancy and OEC oxidation state. The relative affinity of NH_3 and NH_4^+ and the ability to compete with water binding are determined.

The sampling of ammonia binding shows at least 6 binding sites near the OEC, and ammonia will outcompete water for 5 out of 6 sites. Ammonia not ammonium binds to each site. This predicts that the affinity will decrease with pH, as is shown experimentally here. However, only three sites have significant interactions with the OEC. Ammonia binding is weakened by Cl^- through direct competition for one site and indirectly due to the loss of protons on two glutamic acids (E65 and E329), which change the electrostatic field at 2 other sites. The ammonia closest to K317, which is not the direct competitor with Cl^-, may participate in a proton shift from the nearby Lys to create an ammonium : neutral Lys pair. In addition, ammonia bind more tightly when the OEC is in the S_2 $g = 4.1$ state (with Mn1 oxidized) than in the S_2 $g = 2.0$ state where Mn4 is oxidized because of the movement of charge away from its binding sites. Thus, these simulations help explain much of the experimentally observed effects of secondary ammonia binding.

Methods

The 1.9 Å structure of *Thermosynechococcus vulcanus* PSII (PDB ID 3ARC)[1] was used as the starting structure. Calculations were carried out on 20 Å radius spheres containing the following residues (capping residues in parenthesis use only the backbone atoms): *D1 (chain A)*: (57)-58-67-(68), (81)-82-91-(92), (107)-108-112-(113), (155)-156-192-(193), (289)-290-298-(299), (323)-324-344: C-terminus; *CP43 (chain C)*: (290)-291-(292), (305)-306-314-(315), (334)-335-337-(338), (341)-342-(343), (350)-351-358-(359), (398)-399-402-(403), (408)-409-413-(414); *D2 (chain D)*: (311)-312-321-(322), (347)-348-352: C-terminus. The model is centered on the OEC and optimized with DFT-QM/MM in the S_2 $g = 4.1$ redox state (4443, abbreviated as S2_g4.1) and in the S_2 $g = 2.0$ redox state (3444, abbreviated as S2_g2.0).[9] The RMSD between the spheres is <0.035 Å. Two Cl^- ions found in the crystal structure, one near Lys317 and the other near N338 and F339, are retained. In the text, residues discussed without a specified subunit are in the D1 polypeptide.

MCCE calculations were carried out as described previously.[33] Each position and protonation state of a group is called a conformer. The data are primarily reported for calculations using isosteric conformers for the protein, which sample hydroxyl positions, His tautomers and protonation states of all groups at a fixed oxidation state. These were compared with the results found with full rotamer sampling where side chains were built in different rotamers, each one of which has a full panoply of isosteric conformers to sample. The ammonia binding affinities differed by <0.2 kcal mol^{-1} in full and isosteric sampling calculations. Similar negligible differences were found when the calculations were carried out with the sphere docked into the entire PSII complex at pH 7.5 in the absence of Cl^-. Thus, only results of the simpler isosteric runs are reported here. The protein dielectric constant is 4 and the solvent has a dielectric constant of 80 with 150 mM salt. Parse charges[34] are used for the protein and valence charges are used for the OEC.[33] Ammonia charges and radii are given in the ESI.† The OEC is in the S_2 $g = 4.1$ state unless otherwise noted. The Cl^- is either fixed in its position in the initial structure or removed.

Many possible positions for ammonia or ammonium binding near the OEC were subjected to binding analysis. Thus, IPECE[35] was first used to add ammonia to all cavities in the S_2 $g = 4.1$ sphere from which water had been removed and replaced with a high dielectric constant as is routine in Continuum Electrostatics analysis. IPECE added 108 ammonia N, on a 1 Å grid to the cavities. Then rotations around the central N, generates 8(±1) conformers for the protons of each neutral ammonia, 2 conformers for NH_4^+ and 11(±3) NH_2^- conformers.[32] Each ammonia also has an NH_3, NH_4^+ and NH_2^- conformer that represents its having moved out of the protein into water, with a probability that depends on the pH. Six ammonia molecules were found to be bound to the protein in at least 50% of the Monte Carlo accepted microstates, with an ammonia chemical potential equivalent to a solution con-

centration of ≈100 mM.[36] All other ammonias were then removed and the DelPhi electrostatic energies were recalculated, filling cavities with implicit water.[32] The neutral NH_3 in solvent served as the reference for all forms of ammonia. The solution NH_4^+ has free energy equal to pH-pK_a with pK_a = 9.25. Bound NH_4^+ retains the pH dependent energy in addition to the energy of interaction with the protein.[36] MCCE then evaluates the relative affinity of all ammonia conformers, using Grand Canonical Monte Carlo (GCMC) sampling. The ammonia comes to equilibrium with the protein and solvent as a function of concentration and pH.[36]

Ammonia binding is also evaluated in a sphere optimized in the S_2 g = 2.0 state. The atomic coordinates are aligned with the S_2 g = 4.1 coordinates and the six ammonias are transferred into the structure. The ammonias experience no van der Waals clashes in the transfer.

The D2-K317A mutant was generated within MCCE, using the residue completion subroutine, with the Ala keeping the original Lys backbone and beta carbon coordinates. One extra water with 18 conformers for the proton positions was added at the position of the ε carbon of K317.

Explicit waters were added to the positions of the 6 ammonia. Each had 10 different proton positions, providing different orientations to be sampled in the protein. No van der Waals clashes were found.

The MCCE and QM/MM calculations started with the same model sphere cut out of the protein. The computational model of the OEC of PSII was constructed as in our previous reports.[37,38] A more complete description of the QM/MM and DFT calculations is found in the ESI.†

Spinach PSII membranes and *Synechocystis* PCC 6803 PSII core complexes were isolated as described previously.[39–42] EPR spectra were recorded using a Bruker ELEXSYS E500 spectrometer. See the ESI† for additional details of the experimental conditions.

Results

MCCE analysis found six independent ammonia binding sites near the OEC with an affinity in the millimolar range (Fig. 1). These are hydrogen bonded to D2-K317 (Am1, Am2 and Am3), D1-D61 (Am1 and Am6), D1-E65 (Am3 and Am6), the W2 ligand to Mn4 (Am4) or the W3 ligand to Ca^{2+} (Am6). Am2 binds in the Cl^--binding site near D2-K317.

The ammonia binding affinity at these 6 sites was determined as a function of the ammonia chemical potential with and without the chloride near D2-K317 (Table 1, Fig. 2). The distal Cl^- near N338 and F339 was retained. MCCE kept the ionization states of the amino acids in equilibrium with the ammonia, Cl^- and the OEC. Despite the solution pK_a of ammonia being 9.25, all sites bind NH_3 except for Am1, which is hydrogen bonded to D61 and K317. In MCCE calculations, a proton was transferred from K317, so at equilibrium the dominant state is $NH_4^+K317^0D61^-$. This internal proton transfer does not represent a change in overall protonation of the system so it does not impart a pH dependence of the affinity. Rather, it reflects the competition of K317 and ammonia for the proton within the complex electrostatic environment near the OEC. As the intrinsic proton affinity gives Lys a pK_a of 10.4 and ammonia one of 9.25 in water, it does not take a large shift in the relative energy to have K317 transfer its proton to Am1.

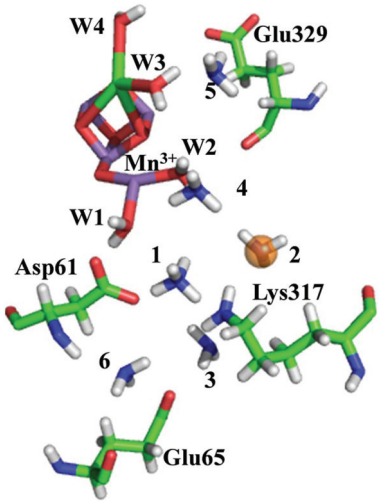

Fig. 1 The 6 ammonias tightly bound in a 20 Å radius sphere cut out of the 3ARC crystal structure centered at the OEC and optimized in the S_2 g = 4.1 state. Am1: 4.1 Å from the dangler Mn (Mn4) and hydrogen bonded to the side-chain oxygen of D61 and N-atom of the D2-K317 side-chain. A proton is transferred from K317 to this ammonium resulting in formation of an ammonium ion (NH_4^+) with a neutral Lys. All other ammonias bind in their neutral state. Am2: competes for the Cl^--binding site, with the ammonia nitrogen hydrogen bonded (2.34 Å) to K317 side chain. Am3: hydrogen bonded to K317 (2.23 Å) as well as to E65 (2.4 Å). Am4: hydrogen bonded to W2 (2.23 Å) and close to W1 (3.03 Å) and Mn4 (4.30 Å), with W2 and W1 being water ligands to Mn4. Am5: is hydrogen bonded to W3 (2.45 Å), a ligand to the OEC Ca^{2+}. Am6: hydrogen bonded to the backbone lying between D61 and E65.

Table 1 Free energy (kcal mol^{-1}) of ammonia (or water) binding to six high affinity binding sites near the OEC

	Am1	Am2	Am3	Am4	Am5	Am6
No Cl^-	−2.2	−1.7	−1.2	−0.8	−1.0	−0.1
With Cl^-	−0.3	–	0.1	−0.2	−0.4	0.4
K317A	−0.9	−0.1	0.4	−0.7	−0.8	0.1
pH 5	0.9	1.7	2.4	2.6	2.3	3.3
pH 6	−0.4	0.4	0.9	1.2	1.0	1.9
pH 7	−1.8	−1.0	−0.6	−0.1	−0.4	0.6
pH 7.5	−2.2	−1.6	−1.2	−0.8	−1.0	−0.1
S_2 g = 2.0	3.2	−1.1	−1.0	−0.9	−1.1	−0.1
Water affinity	2.9	3.0	3.5	3.5	3.2	3.7
W2 protonated	11.2	−1.5	−1.7	−0.9	−1.0	−0.2
QM/MM (W2 protonated)	10.3	1.4	0			

The free energy of binding is obtained from the fraction of each ammonia bound as a function of ammonia chemical potential given $\Delta G^\circ = -RT \ln K_d$. If not explicitly stated, the calculations are carried out with MCCE in the sphere with the OEC optimized in the S_2 g = 4.1 (4443) redox state at pH = 7.5, with the Cl^- near D2-K317 removed.

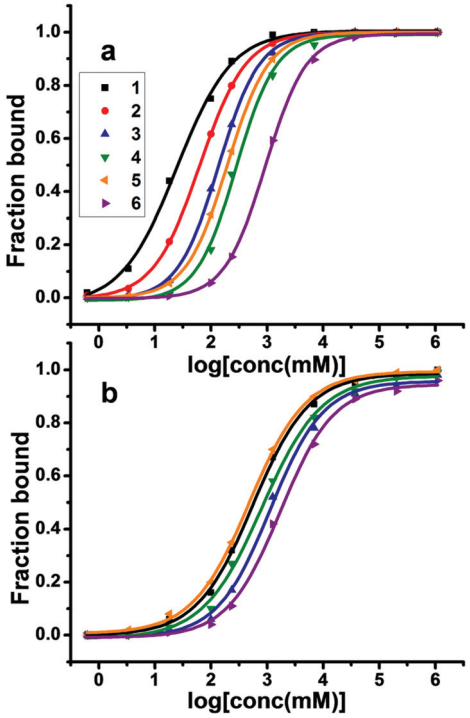

Fig. 2 Ammonia binding as a function of chemical potential in: (a) absence and (b) presence of chloride. The affinity of all six sites is evaluated in one calculation.

DFT geometry optimization also favors proton transfer from D2-K317 to Am1, forming NH_4^+ in the absence of chloride (see ESI†). In an analogous QM/MM calculation, the proton remains on K317 but with a strong hydrogen bond between K317 and Am1. Thus, the different calculation techniques agree the ammonia–Lys pair will hold the proton, but the states with the ammonia or the Lys 'owning' the proton may be close in energy. DFT and MCCE calculations find that in the presence of chloride, there is a strong hydrogen bond between D2-K317 and the chloride that stabilizes the $NH_3{}^0K317^+$ state.

In the absence of Cl^-, the affinity of ammonia ranges from −2.2 to −0.1 kcal mol^{-1} at pH 7.5 (Table 1). With Cl^- present all binding sites have fairly similar, weaker affinities. Am2 is absent with Cl^- present, as it is a true competitive inhibitor of Cl^-, with both binding to the same site. In the presence of Cl^-, the proton shift from K317 to Am1 is no longer favored. Cl^- also changes the ammonia affinity through its influence on the ionization states of E65, E329 and K317. In the absence of Cl^-, these acids are more ionized, enhancing the electrostatic field that contributes to the ammonia affinity.

The relative stability of the Am1–Am3 sites was compared to that found using QM/MM calculations. The results for Am2 and Am3 are in reasonable agreement; however, the affinity of Am1, paired with D2-K317, is greatly reduced. This difference results from the charge on water 2 (W2, a primary ligand to Mn4), which is fixed to be neutral in the QM/MM calculations and becomes a hydroxyl when freely sampled in the MCCE analysis in the S_2 state. The proton transfer from K317 to Am1, is strongly stabilized by the deprotonated W2. If W2 is constrained to remain protonated in the MCCE calculation, the binding affinities for the three ammonias are in good agreement when the classical MCCE and QM/MM methods are compared (Table 1). The protonation state of this water is not well established, with computation studies suggesting it is ionized[43–47] or not.[8,48–50]

Effect of ammonia on the S_2 spin isomer population

Experimental findings show that secondary ammonia binding is associated with stabilization of the S_2 g = 4.1 redox state, (4443, where Mn1 is oxidized) and the loss of the multiline, S_2 g = 2.0 state (3444, where the dangler Mn4 is oxidized) (Fig. S2†). Calculations with the OEC in the S_2 g = 2.0 state, show the affinity for Am1 is decreased by 5.3 kcal mol^{-1}. Thus, ammonia will not bind here in the g = 2.0 state. The Am2 affinity decreases by 0.5 kcal mol^{-1}. The affinity of ammonia at sites 3–6 is unaffected. The stability difference of the two spin states has been estimated experimentally to be as little as 0.7 kcal mol^{-1},[51] so even small changes in the environment could influence the equilibrium between the two spin isomers. The changes in affinity are the same when the OEC is fixed in the 3444 state when the OEC geometry is optimized in S_2 g = 4.1 or S_2 g = 2.0 states (Table S2†). Thus, it is the movement of the positive charge from Mn1 to Mn4 that reduces the affinity of Am1 and Am2.

There is also ≈0.35 more protonation of E65 and E329 in the S_2 g = 2.0 spin isomer. This can be compared with the effect of Cl^- which leads to ≈0.95 increase in protonation at these same sites. Thus, the charge shift in the OEC may influence the electrostatic environment for the secondary ammonia in a manner similar to that found by Cl^- binding (see Table S1†).

pH dependence of ammonia binding

At pH 7.5, upon addition of 22 mM NH_4^+ ($[NH_3]$ = 0.4 mM) followed by illumination at 200 K, a g = 4.1 signal is observed in the ammonia-treated *Synechocystis* PCC 6803 PSII samples corresponding to the S_2, S = 5/2 spin isomer (Fig. 3, spectrum A). This is characteristic of ammonia binding at the secondary site.[19,52] However, upon addition of 700 mM NH_4^+ at pH 6.0 ($[NH_3]$ = 0.4 mM) followed by illumination under similar conditions, no signal is observed at g = 4.1 (Fig. 3, spectrum B). Thus, the secondary binding site of ammonia, responsible for stabilization of the g = 4.1 signal (S = 5/2 spin isomer) in the S_2 state, is pH dependent, being stabilized at higher pH. There are additional EPR hyperfine line features of the g = 4.1 signal in ammonia-treated oriented PSII samples which are not observed in the native g = 4.1 signal of spinach PSII. This indicates there are subtle differences between the native and ammonia treated g = 4.1 state.[53,54] However, there are no major differences found with addition of ammonia, which strongly suggests that the g = 4.1 signal arises from the same spin state.

MCCE ammonia affinity calculations have been performed between pH 5 and 7.5. The relative affinities of ammonias decrease significantly at lower pH. At pH ≤ 6, E65 and E329

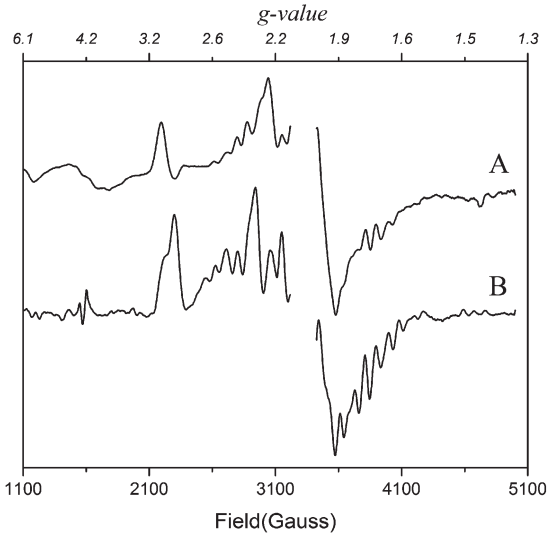

Fig. 3 S_2 state light-minus-dark spectra of NH_3-treated *Synechocystis* PCC 6803 PSII core complexes: (A) 0.4 mM NH_3 at pH 7.5 and (B) 0.4 mM NH_3 ammonia at pH 6.0.

are mostly protonated, D61 is not fully deprotonated and there is less proton transfer from K317 to Am1. By pH 7.5, these acidic residues are fully ionized, yielding a tighter binding affinity for Am1, Am2 and Am3. However, the major contributor to the tighter affinity of ammonia at high pH is simply the increasing concentration of the NH_3 form (Fig. 4).

The pH dependence provides another example of the antagonistic effect of Cl^- and ammonia binding. Cl^- binding is favored at low pH, while ammonia binding is favored at high pH. Calculations show Am2 replaces the chloride ion as the pH is raised, while the Cl^- binds more tightly at lower pH.

The role of K317 in ammonia binding

Experimental results[19] show that the effects of the secondary ammonia on the OEC is lost in PSII with a K317A substitution.

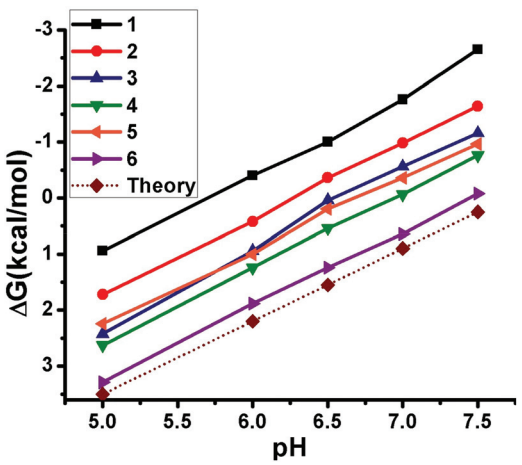

Fig. 4 pH dependence of ammonia binding. The relative chemical potential of the NH_3 state of ammonia is given for comparison.

The relative ammonia affinity has been calculated for K317A PSII in the absence of chloride. Am1, Am2 and Am3 are less tightly bound in the mutant, making them candidates for the active secondary ammonia positions. The affinities of the other ammonias are not sensitive to the K317 mutation.

Competition between ammonia and water in the ammonia-binding sites

In solution, ammonia will compete with water for the binding sites studied here. The affinity of explicit water in the positions of the ammonias is compared with that of ammonia itself. With the concentration of ammonia in the 100 mM range and a water concentration of 55 M, water molecules successfully compete only for position 6 (see Table 1).

Discussion

Six binding sites were found for ammonia near the OEC indicating that there need not be a unique ammonia binding site in the second coordination sphere around the OEC. All six binding sites are easily accessible to solvent as they are in the established water channels.[55] Am1, 3 and 6 are in the proton exit channel, Am2 and 4 are in the broad channel, and Am5 is in the large channel. The question is which of the possible binding sites is most likely responsible for the ammonia effects observed in experiments, including the competitive inhibition with Cl^-,[13] the strong preference for the S_2 g = 4.1 spin isomer,[19] the sensitivity to the presence of D2-K317,[19] and tighter binding at higher pH (Fig. 3).

The most promising sites that perturb activity bind Am1 and Am2 and to a lesser extent Am3. Positions 1–3 are all strongly inhibited by Cl^- and have similar dependencies on the OEC S_2 spin state and the presence of K317. In contrast, positions 4–6 bind more weakly and are only weakly dependent on the concentration of Cl^-, the D2-K317A substitution or the S_2 spin state. However, the binding of ammonia to sites 4–6 are a reminder that small molecules may populate water cavities in proteins without significant changes in function.

The MCCE calculations would favor Am1 as the best candidate for producing the observed effects due to binding of ammonia to the secondary site. It is the tightest binding ammonia, its affinity is dependent on the concentration of Cl^-, and it is sensitive to pH, to the D2-K317A substitution and to different spin isomers of the S_2 state. In addition, FTIR measurements show NH_3 altered the spectral region (1450–1300 cm^{-1}) of the symmetric carboxylate stretching modes,[17,56] which is consistent with proton transfer from D2-K317 to Am1. Changes in the asymmetric and symmetric COO^- stretch are also seen, which could arise from the nearby Am1 changing the D61 COO^- stretching frequency. However, Am1 binding relies on the W2 ligand of Mn4 being a hydroxyl. In calculations with a protonated W2, Am2 becomes the most likely candidate to produce the observed ammonia-binding effects. However, as Am2 remains in the NH_3 form it cannot be the source of an NH_4^+ FTIR signal. It should be recognized

that the experiments would be consistent with Am1 and Am2 both contributing to the ammonia effects.

Cl^- and ammonia are rather different types of small molecules that nevertheless compete to influence the OEC. The simplest explanation for their competitive effects is that they are bound in the same site,[15,19] an assumption that is tested by the simulations presented here. Am2 competes directly with Cl^- for one binding site. However, Cl^- decreases the affinity of Am1 and Am3 indirectly. Cl^- increases the protonation of acidic residues (E65, E329 and D61) which weakens their H-bonds with ammonia. In addition, both the MCCE and DFT calculations show that proton transfer from K317 to Am1 is suppressed by the presence of Cl^-, which also weakens its affinity.

Another consideration with regard to the relative importance of ammonia in different positions, is that the secondary ammonia is the likely source for the primary ammonia that is bound in the higher S states. Am1 sits close to D61 and K317, which may facilitate its becoming a ligand of Mn4 either by exchange with W1 or W2 or adding as an extra ligand.[9] The Am1 $NH_4^+K317^0D61^-$ state includes a strong salt-bridge with D61, which could make D61 a weaker proton acceptor from the OEC and, therefore, could suppress oxygen evolution. Am2 is also well placed to move into the OEC primary site. In contrast, Am3 is farther away from the OEC and so is not as well situated to transfer into the primary ammonia-binding site.

Experimental results show that ammonia binds to the secondary site at higher pH(= 7.5) and not at lower pH(= 6) (Fig. 3). At pH 7.5, only Am1 and Am2 are calculated to bind within the experimental range of concentration. None of the six ammonias bind tightly at pH 6 so each would be displaced by water. At higher pH, titratable residues close to Am1 or Am2, such as D61 and E65, become deprotonated increasing the ammonia affinity. Thus, the simulations help to explain the experimental results.

Conclusions

Six positions were identified for ammonia binding in the secondary coordination shell of the OEC of PSII. The sites were evaluated by their sensitivity to parameters that affect ammonia binding as determined by experiments. These include the Cl^- concentration, pH, the presence of the D2-Lys317 residue and the different spin isomers of the S_2 state. Am1 is involved with in an ion pair with Lys317 and is well poised to move to the primary ammonia position, becoming a direct ligand to Mn4. Am2 is a competitive inhibitor of Cl^-, while Am1 and Am3 indirectly compete with Cl^- through the nearby E65 residue, which becomes increasingly protonated in the presence of Cl^-. In contrast, ammonia at positions 4–6 are little influenced by Cl^-, the OEC spin state or D2-K317 substitutions. Thus, the calculations show there may be multiple positions for binding of a molecule with a small dipole such as ammonia, some which can be seen to change the behavior of the protein, while others may be silent.

Conflicts of interest

There are no conflicts to declare.

Acknowledgements

The authors acknowledge support by the U.S. Department of Energy, Office of Science, Office of Basic Energy Sciences, Division of Chemical Sciences, Geosciences, and Biosciences, Photosynthetic Systems. Experimental work was funded by DE-FG02-05ER15646 (G. W. B.) and computational studies by DESC0001423 (M. R. G. and V. S. B.). M. R. G. also acknowledges infrastructure support from the National Institute on Minority Health and Health Disparities (Grant 8G12MD007603) from the National Institutes of Health. M.A. acknowledges a Consolidator Grant COMOTION (ERC-Küpper-614507) from the European Research Council. We would like to acknowledge helpful discussions with Witold Szeijgis.

References

1 Y. Umena, K. Kawakami, J.-R. Shen and N. Kamiya, *Nature*, 2011, **473**, 55–60.
2 B. Kok, B. Forbush and M. McGloin, *Photochem. Photobiol.*, 1970, **11**, 457–475.
3 J. P. McEvoy and G. W. Brudvig, *Chem. Rev.*, 2006, **106**, 4455–4483.
4 N. Cox, D. A. Pantazis, F. Neese and W. Lubitz, *Acc. Chem. Res.*, 2013, **46**, 1588–1596.
5 J. R. Shen, *Annu. Rev. Plant Biol.*, 2015, **66**, 23–48.
6 P. E. M. Siegbahn, *Chem. – Eur. J.*, 2006, **12**, 9217–9227.
7 M. Askerka, D. J. Vinyard, G. W. Brudvig and V. S. Batista, *Biochemistry*, 2015, **54**, 5783–5786.
8 M. Askerka, G. W. Brudvig and V. S. Batista, *Acc. Chem. Res.*, 2017, **50**, 41–48.
9 D. J. Vinyard and G. W. Brudvig, *Annu. Rev. Phys. Chem.*, 2017, **68**, 101–116.
10 M. Retegan, V. Krewald, F. Mamedov, F. Neese, W. Lubitz, N. Cox and D. A. Pantazis, *Chem. Sci.*, 2016, **7**, 72–84.
11 V. L. Pecoraro, M. J. Baldwin, M. T. Caudle, W. Y. Hsieh and N. A. Law, *Pure Appl. Chem.*, 1998, **70**, 925–929.
12 G. W. Brudvig, *Philos. Trans. R. Soc. London, Ser. B*, 2008, **363**, 1211–1219.
13 P. O. Sandusky and C. F. Yocum, *Biochim. Biophys. Acta*, 1984, **766**, 603–611.
14 W. F. Beck and G. W. Brudvig, *Biochemistry*, 1986, **25**, 6479–6486.
15 M. Perez Navarro, W. M. Ames, H. Nilsson, T. Lohmiller, D. A. Pantazis, L. Rapatskiy, M. M. Nowaczyk, F. Neese, A. Boussac, J. Messinger, W. Lubitz and N. Cox, *Proc. Natl. Acad. Sci. U. S. A.*, 2013, **110**, 15561–15566.
16 P. H. Oyala, T. A. Stich, R. J. Debus and R. D. Britt, *J. Am. Chem. Soc.*, 2015, **137**, 8829–8837.

17 M. Tsuno, H. Suzuki, T. Kondo, H. Mino and T. Noguchi, *Biochemistry*, 2011, **50**, 2506–2514.
18 P. O. Sandusky and C. F. Yocum, *Biochim. Biophys. Acta*, 1986, **849**, 85–93.
19 D. J. Vinyard, M. Askerka, R. J. Debus, V. S. Batista and G. W. Brudvig, *Biochemistry*, 2016, **55**, 4432–4436.
20 W. F. Beck and G. W. Brudvig, *Chem. Scr.*, 1988, **28A**, 93–98.
21 C. F. Yocum, *Coord. Chem. Rev.*, 2008, **252**, 296–305.
22 A. Guskov, J. Kern, A. Gabdulkhakov, M. Broser, A. Zouni and W. Saenger, *Nat. Struct. Mol. Biol.*, 2009, **16**, 334–342.
23 K. Kawakami, Y. Umena, N. Kamiya and J. R. Shen, *Proc. Natl. Acad. Sci. U. S. A.*, 2009, **106**, 8567–8572.
24 R. Pokhrel, I. L. McConnell and G. W. Brudvig, *Biochemistry*, 2011, **50**, 2725–2734.
25 A. W. Rutherford, *Trends Biochem. Sci.*, 1989, **14**, 227–232.
26 I. Rivalta, M. Amin, S. Luber, S. Vassiliev, R. Pokhrel, Y. Umena, K. Kawakami, J. R. Shen, N. Kamiya, D. Bruce, G. W. Brudvig, M. R. Gunner and V. S. Batista, *Biochemistry*, 2011, **50**, 6312–6315.
27 M. Amin, R. Pokhrel, G. W. Brudvig, A. Badawi and S. S. A. Obayya, *J. Phys. Chem. B*, 2016, **120**, 4243–4248.
28 R. Pokhrel, R. J. Service, R. J. Debus and G. W. Brudvig, *Biochemistry*, 2013, **52**, 4758–4773.
29 D. A. Pantazis, W. Ames, N. Cox, W. Lubitz and F. Neese, *Angew. Chem., Int. Ed.*, 2012, **51**, 9935–9940.
30 P. van Vliet and A. W. Rutherford, *Biochemistry*, 1996, **35**, 1829–1839.
31 T. Ono, J. L. Zimmerman, Y. Inoue and A. W. Rutherford, *Biochim. Biophys. Acta*, 1986, **851**, 193–201.
32 Y. Song, J. Mao and M. R. Gunner, *J. Comput. Chem.*, 2009, **30**, 2231–2247.
33 M. Amin, L. Vogt, W. Szejgis, S. Vassiliev, G. W. Brudvig, D. Bruce and M. R. Gunner, *J. Phys. Chem. B*, 2015, **119**, 7366–7377.
34 D. J. Tannor, B. Marten, R. Murphy, R. A. Friesner, D. Sitkoff, A. Nicholls, B. Honig, M. Ringnalda and W. A. Goddard III, *J. Am. Chem. Soc.*, 1994, **116**, 11875–11882.
35 Y. Song, J. Mao and M. R. Gunner, *Biochemistry*, 2003, **42**, 9875–9888.
36 Y. Song and M. R. Gunner, *J. Mol. Biol.*, 2009, **387**, 840–856.
37 R. Pal, C. F. Negre, L. Vogt, R. Pokhrel, M. Z. Ertem, G. W. Brudvig and V. S. Batista, *Biochemistry*, 2013, **52**, 7703–7706.
38 M. Askerka, J. Wang, G. W. Brudvig and V. S. Batista, *Biochemistry*, 2014, **53**, 6860–6862.
39 H.-A. Chu, R. J. Debus and G. T. Babcock, *Biochemistry*, 2001, **40**, 2312–2316.
40 M. Strickler, L. Walker, W. Hillier and R. Debus, *Biochemistry*, 2005, **44**, 8571–8577.
41 D. A. Berthold, G. T. Babcock and C. F. Yocum, *FEBS Lett.*, 1981, **134**, 231–236.
42 W. F. Beck, J. C. de Paula and G. W. Brudvig, *Biochemistry*, 1985, **24**, 3035–3043.
43 A. Galstyan, A. Robertazzi and E. W. Knapp, *J. Am. Chem. Soc.*, 2012, **134**, 7442–7449.
44 P. E. M. Siegbahn, *Phys. Chem. Chem. Phys.*, 2014, **16**, 11893–11900.
45 D. A. Pantazis, W. Ames, N. Cox, W. Lubitz and F. Neese, *Angew. Chem., Int. Ed.*, 2012, **51**, 9935–9940.
46 M. Shoji, H. Isobe, S. Yamanaka, M. Suga, F. Akita, J. R. Shen and K. Yamaguchi, *Chem. Phys. Lett.*, 2015, **623**, 1–7.
47 I. Ugur, A. W. Rutherford and V. R. Kaila, *Biochim. Biophys. Acta, Bioenerg.*, 2016, **1857**, 740–748.
48 M. Askerka, D. J. Vinyard, J. M. Wang, G. W. Brudvig and V. S. Batista, *Biochemistry*, 2015, **54**, 1713–1716.
49 R. Chatterjee, G. Han, J. Kern, S. Gul, F. D. Fuller, A. Garachtchenko, I. D. Young, T.-C. Weng, D. Nordlund, R. Alonso-Mori, U. Bergmann, D. Sokaras, M. Hatakeyama, V. K. Yachandra and J. Yano, *Chem. Sci.*, 2016, **7**, 5236.
50 S. Petrie, R. J. Pace and R. Stranger, *Angew. Chem., Int. Ed.*, 2015, **54**, 7120–7124.
51 D. J. Vinyard, S. Khan, M. Askerka, V. S. Batista and G. W. Brudvig, *J. Phys. Chem. B*, 2017, **121**, 1020–1025.
52 A. Boussac, M. Sugiura, Y. Inoue and A. W. Rutherford, *Biochemistry*, 2000, **39**, 13788–13799.
53 D. H. Kim, R. D. Britt, M. P. Klein and K. J. Sauer, *J. Am. Chem. Soc.*, 1990, **112**, 9389–9391.
54 D. H. Kim, R. D. Britt, M. P. Klein and K. Sauer, *Biochemistry*, 1992, **31**, 541–547.
55 S. Vassiliev, P. Comte, A. Mahboob and D. Bruce, *Biochemistry*, 2010, **49**, 1874.
56 H. A. Chu, Y. W. Feng, C. M. Wang, K. A. Chiang and S. C. Ke, *Biochemistry*, 2004, **43**, 10877–10885.